



## Smooth particle hydrodynamics simulation of surface coating

P.J. Reichl <sup>a,\*</sup>, P. Morris <sup>a</sup>, K. Hourigan <sup>a</sup>, M.C. Thompson <sup>a</sup>, S.A.T. Stoneman <sup>b</sup>

<sup>a</sup> *Fluid-dynamics Laboratory for Aeronautical and Industrial Research (F.L.A.I.R.), Department of Mechanical Engineering, Monash University, Clayton, Vic. 3168, Australia*

<sup>b</sup> *Department of Civil Engineering, University of Wales, Swansea, UK*

Received 1 July 1997; received in revised form 15 March 1998; accepted 15 March 1998

---

### Abstract

The simulation of plane impinging jets using the Lagrangian technique of smooth particle hydrodynamics is presented. In Section 1 the impingement of a plane jet onto a stationary surface is considered for Reynolds numbers 800, 4000, 8000 and Froude number 4. For each case, the height of the associated streams is measured and compared with both experimental and theoretical results. The agreement between these results is found to be close for most impingement angles. In the second section, impingement onto a moving surface is considered for Reynolds numbers of 50 and 800 and Froude numbers of 1 and 4. The preliminary results show that the moving surface can lead to some spatial height variation in at least one of the streams. © 1998 Elsevier Science Inc. All rights reserved.

---

### 1. Introduction

Free surface flows occur in a wide variety of situations in both industry and the environment. However, due to the problems associated with the implementation of appropriate boundary conditions on a surface whose position is constantly changing, such flows are often arduous to model numerically.

Of specific importance is the study of impinging jets, the use of which is widespread throughout many industries. For example, impinging jets are frequently encountered in VTOL aircraft, fluid mixing, fuel filling, combustors and ejectors, ventilation, electronic component cooling, in the annealing of non-ferrous sheets, and in the cutting of rock in the mining industry.

Of particular concern in the present study is the use of impinging jets in the coating of surfaces, which is often widespread in industries associated with the application of corrosion inhibiting agents, paints and dyes, magnetic films on tapes, and laminates on paper products. In extrusion coating, for example, a thin layer of fluid is deposited onto a moving substrate, with the liquid then solidifying as it passes through an oven. In these situations, the aim is to achieve a uniformity in the coating thickness and thus ensure that no undulations or voids are present in the final product.

From a numerical stand-point, what often makes coating flows difficult to model is the fact that the region of space occupied by the flowing liquid is not always known in advance, but is

---

\* Corresponding author. Fax: +61 3 9905 9639; e-mail: paul@gauss.eng.monash.edu.au.

itself part of the solution of the hydrodynamic equations. The plethora of different coating techniques only helps to reinforce some of the practical difficulties that are associated with coating flows. Ruschak [1] describes in detail some of the problems that are often encountered.

Smooth particle hydrodynamics (SPH) is a Lagrangian technique, and as a result it requires no grid. Its in-built ability to automatically track the position of the free surface, while also handling any spatial surface gradient, may therefore make this scheme a useful tool in the study of free surface behavior. This technique was first utilised to investigate complex astrophysical phenomena [2,3]. However, more recently it has been applied to almost incompressible flows, with Monaghan [4], Thompson et al. [5] and Takeda et al. [6] considering SPH's applicability to a number of test problems in which the fluid was assumed to be nearly incompressible (that is, fluctuation in density were limited to order 1%). In addition, its roots in astrophysics have ensured its application to flows involving magnetic fields, and while such flows are not investigated here, the potential to exploit this knowledge for applications involving magnetic films is still untapped.

The present work is divided into two parts, with the first looking at the heights of the two streams associated with the impingement of a plane jet onto a stationary flat surface, while the second involves an investigation with a moving surface. The problems to be examined here provide a further test of SPH's ability to handle free surface flows. In the first case, the heights of the two streams from an impinging plane jet onto a stationary plate will be compared with the results of experiment and theory. This problem is considered because it enables the incorporation of free surfaces, while still remaining relatively simple, and also allows for both experimental and theoretical validation of the results. The second case is considered because of its importance to many industrial applications.

Section 2 highlights the basic formulation and governing equations, while Section 3 will look at the results and their discussion.

## 2. Formulation

The governing equations in SPH determine the characteristics of each of the interpolating points or particles. These equations will now be presented.

### 2.1. Momentum

The momentum equation is obtained after applying theory of integral interpolants to the modified Euler equation,

$$\frac{dv}{dt} = -\frac{1}{\rho} \nabla(P + P_V) + F_{ex}, \quad (1)$$

where  $P_V$  is an artificial viscous pressure [7].

The resulting momentum equation for each interpolating point denoted by the index  $i$ , is then given by

$$\frac{dv_i}{dt} = -\sum_{j=1}^N m_j \left( \frac{P_i}{\rho_i^2} + \frac{P_j}{\rho_j^2} + v_{ij} \right) \nabla_i W_{ij} + F_{ex}, \quad (2)$$

where  $v_{ij}$  represents the artificial viscosity.

#### 2.1.1. Artificial viscosity

The artificial viscosity used here is that given in [8] which is as follows:

$$v_{ij} = \begin{cases} \frac{-\alpha h c \mu_{ij} + \beta h^2 \mu_{ij}}{\rho_{av}}, & \mathbf{v}_{ij} \cdot \mathbf{r}_{ij} < 0, \\ 0, & \mathbf{v}_{ij} \cdot \mathbf{r}_{ij} > 0, \end{cases} \quad (3)$$

where

$$\mu_{ij} = \frac{\mathbf{v}_{ij} \cdot \mathbf{r}_{ij}}{|\mathbf{r}_{ij}|^2 + \eta^2},$$

which has been shown to conserve both discrete linear and angular momentum.

In the above expression,  $\alpha$  and  $\beta$  are both constants. For the almost incompressible case being examined here, we may set  $\beta = 0$ . The other parameter,  $\eta$ , is simply a small constant chosen so as to ensure that the denominator remains non-zero; in this case it is selected to be  $0.01h^2$ . The effective kinematic viscosity of the fluid is then proportional to  $\alpha hc$ , with the constant of proportionality being dependent upon the interpolation kernel; for the cubic spline and quintic spline kernels used here, this constant is found to be  $1/8$  (see [9]).

Alternative viscosity models are prescribed in [6,10].

## 2.2. Continuity

“Incompressible” SPH requires a small but finite degree of compressibility, and as a result the density at each point will vary slightly.

Although the density can be expressed directly as a sum involving the smoothing kernel, it is more desirable when attempting to model free surfaces to use the continuity equation which gives

$$\frac{d\rho_i}{dt} = \sum_{j=1}^N \rho_j v_{ij} \nabla_i W_{ij}. \quad (4)$$

This is because this formulation does not lead to smoothing of the discontinuous density change at the free surface.

## 2.3. Equation of state

In order to determine the value of the pressure at each point, an equation of state is required which links the pressure to a variable, or series of variables which are already known.

The equation of state used here is that given by Batchelor [11], with the modifications given in [5],

$$P = P_0 \left( \left( \frac{\rho}{\rho_0} \right)^\gamma - 1 \right). \quad (5)$$

In the investigation undertaken here,  $\gamma$  was, as in [4,5], chosen to be 7.

## 2.4. Kernel

From the momentum and continuity equations (2) and (4), it can be seen that the properties for each particle are dependent upon those of all the other particles. However, since it is the choice of the interpolating kernel that affects the degree to which the surrounding particles interact with one another, it is practical to select an appropriate kernel, such that only neighbouring particles exert any influence.

Two different kernels were used in this investigation, both having the property of compact support (that is, the kernel has a finite range in which it possesses a non-zero value). The kernels used were the cubic spline kernel which is given in [12] and the quintic spline kernel of [13]. It

should be noted that both kernels should produce results of accuracy  $O(h^2)$ , where  $h$  is the smoothing length.

### 2.5. Boundary forces

The boundary forces used in the present study consisted of either a Lennard–Jones force (which is described in [4]), or a system of multiple layers of particles.

The Lennard–Jones force, in the absence of an additional viscous model for boundary behavior, can only be used on its own in cases in which the boundaries are assumed to be free slip. For no slip boundary conditions, it is necessary to employ a particle boundary arrangement.

## 3. Results and discussion

### 3.1. Stationary plate

The simulation of an impinging jet over a range of orientation angles of the jet to the vertical, was investigated for the following Reynolds number and Froude number combinations.

$$\begin{aligned} \text{Re} &= 800, \text{Fr} = 4.0, \\ \text{Re} &= 4000, \text{Fr} = 4.0, \\ \text{Re} &= 8000, \text{Fr} = 4.0. \end{aligned}$$

The Froude number, which in this case is the dominant parameter governing the behaviour of the system, was chosen to be 4.0 to match the experimental results which were performed at  $\text{Re} \approx 6400$  and  $\text{Fr} = 4.0$ .

The basic setup of the numerical system involved a series of particles being ejected from a non-interfering nozzle with a uniform velocity profile. The profile was assumed to be uniform for ease of numerical implementation. The Reynolds and Froude number values were then based on the initial jet velocity and the nozzle width.

For cases in which the boundary consisted of a series of particles, either two or three layers of particles were arranged to fit the boundary. These boundary particles were then fixed in space, with only their density being allowed to vary. The density of the boundary particles was permitted to change so as to allow the boundary to respond to any fluctuation in the pressure associated with the motion of the fluid particles. In this case the boundary better captures the interface between the fluid and solid wall.

The resolution of the system is dependent upon the smoothing length and hence upon the number of particles. For all the cases investigated here, the smoothing length,  $h$ , was chosen to be 1.2 times the particle separation. However, particles of varying smoothing lengths, and hence resolution, could have been used. In compressible flows, such as those that often occur in astrophysical situations, automatic variation is possible; however, in the incompressible case it is not such an easy task, and as a result a fixed resolution was used.

For the simulations involving the stationary plate, approximately 25,000 particles were used (50 particles across the inlet). For the entire range of Reynolds numbers investigated, the boundary plate was modelled with a Lennard–Jones force, and the cubic spline kernel was used.

In addition for the  $\text{Re}=800$  case, the boundary was also modelled with layers of particles, and both the cubic spline and quintic spline kernels were used. In this situation, different kernels and boundaries were adopted in order to test the sensitivity of the results to the type of kernel and boundary employed. The results of such a comparison indicate that at least for the case of an impinging jet, the type of kernel and boundary used has little influence on the final result.

For each of the Reynolds number combinations, the heights of the upstream and downstream flows were measured for the angles of 10–80°, at 10° increments.

Fig. 1 shows an example of the experimental findings, which were undertaken at Swansea, for an injection angle of 40°, with Fig. 2 illustrating the equivalent numerical result.

In order to validate the SPH results, a comparison with theory and experiment was undertaken. The results of such a comparison are highlighted in Figs. 3 and 4 which show a good agreement between the numerical, experimental and theoretical results. Note that all the numerical results in Figs. 3 and 4 have been time averaged so as to reduce any inherent transient behaviour.

The experimental results were measured directly from blown up photographs, and have as a consequence an error associated with them.

In order to measure the heights of the streams in the numerical case, each stream was divided up into a number of bins, and the maximum particle height in each bin was then averaged to give a final result, with the uncertainty of such a result being approximately  $O(h)$ .

The theoretical results were obtained via the application to a control volume of Bernoulli's equation, along with a simple mass and momentum balance. This theoretical result was then adjusted in order to take into account that the resulting wall impingement angle alters due to the effect of gravity. This adjustment was made on the basis of free fall arguments, and subsequently has some degree of error associated with it. (The equations used to obtain this result are given in Appendix A).

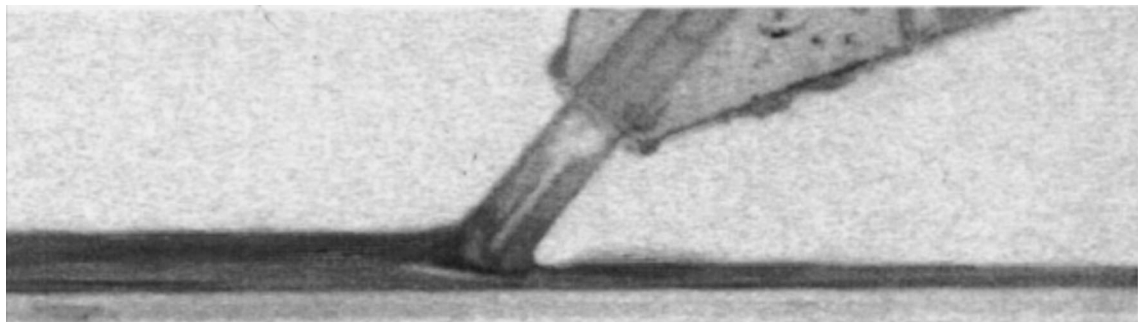


Fig. 1. Experimental visualisation of an impinging jet onto a stationary surface, for an injection angle of 40°;  $Re = 6400$  and  $Fr = 4.0$ .

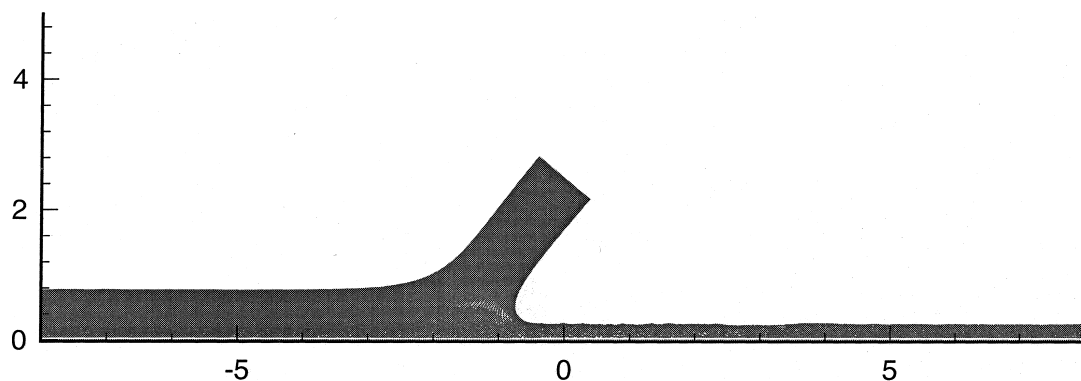


Fig. 2. Predicted flow pattern from the SPH simulation of an impinging jet onto a stationary surface at an injection angle of 40°;  $Re = 800$  and  $Fr = 4.0$ .

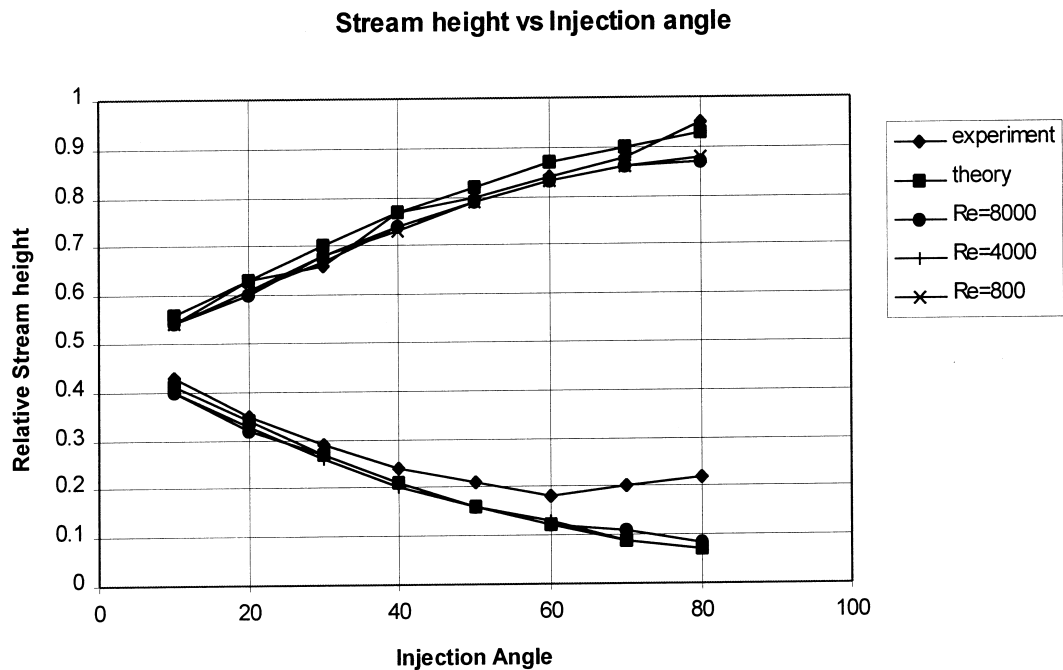


Fig. 3. Comparison of stream heights for the numerical, experimental and theoretical results; boundary = Lennard-Jones, kernel = cubic spline.

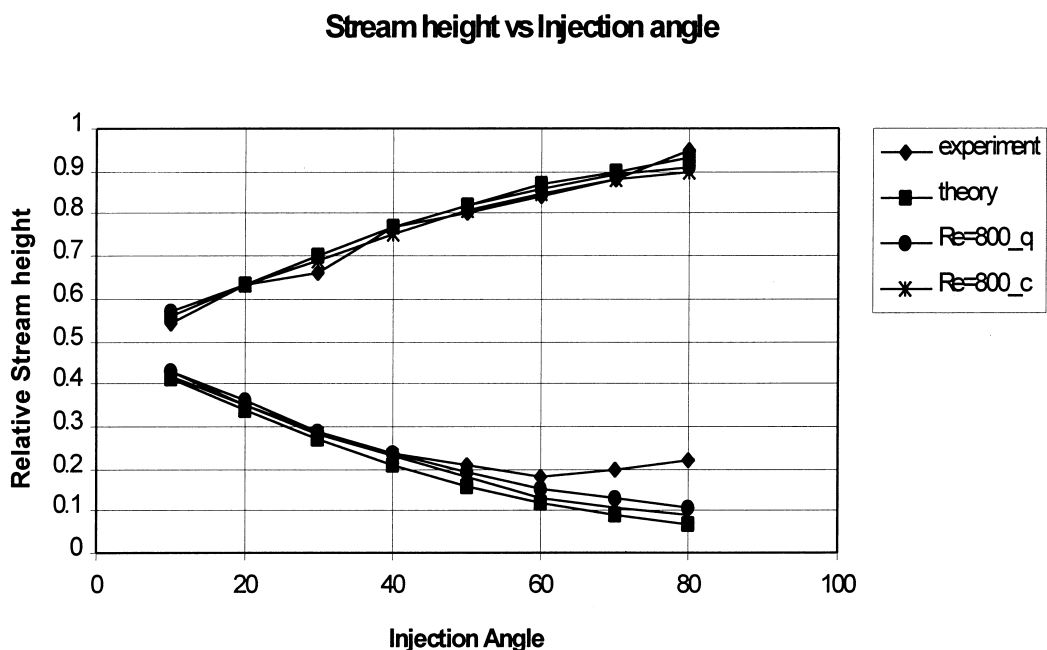


Fig. 4. Comparison of stream heights for the numerical, experimental and theoretical results using different kernels; (\_c = cubic spline, \_q = quintic spline), boundary = particle arrangement.

In order for SPH to accurately simulate a real fluid, a minimum number of particles are required so as to ensure that they adequately model a continuum. For the simulation of the jet at all Reynolds numbers, the number of particles in the downstream flow for angles greater than approximately  $60^\circ$  was relatively small; and as a consequence the results for such cases have a higher degree of uncertainty associated with them. Indeed for the higher Reynolds number cases,  $Re=4000$  and  $8000$ , some break up or scattering was observed, and it was necessary in these situations to filter out the relatively few scattered particles, especially at larger angles.

The agreement between the results in Figs. 3 and 4 is close up until about  $50^\circ$ , at which point for the thinner of the two streams, the experimental results tend to deviate away from those obtained from theory and numerical simulation.

A possible explanation for this deviation is that the error associated with the measuring of the experimental results will tend to be magnified for cases in which the stream height is thinner, and as a consequence the experimental results become less meaningful in this situation. The effect of parallax errors will also become more dominant in situations in which the stream height is small. In addition, the numerical results are less meaningful when there are a small number of particles simulating the fluid, and hence the accuracy of both the experimental and numerical results diminish in this region.

### 3.2. Moving plate

The initial investigation involving the moving plate was undertaken at a Reynolds number of  $800$  and a Froude number of  $4.0$ . Numerically the setup was similar to the stationary case, except that the particles making up the boundary were driven with the desired velocity (the driving velocity being from right to left in Figs. 5–8).

The behaviour of the impinging jet was then investigated for a plate velocity of  $0.5$  times the initial jet velocity. Figs. 5 and 6 show the behaviour of the jet for different angles. What appears to be evident from these preliminary simulations is the presence of undesirable and somewhat unphysical voids; this is particularly the case in Fig. 6.

This erratic behaviour is most likely due to a lack of resolution, especially at the boundary layer, and as a consequence these results must be viewed with a measured degree of scepticism.

Another investigation involving a higher resolution was then carried out at a Reynolds number of  $50$ . However in this case two Froude numbers were considered, these being  $1$  and  $4$ . These results are shown in Figs. 7 and 8.

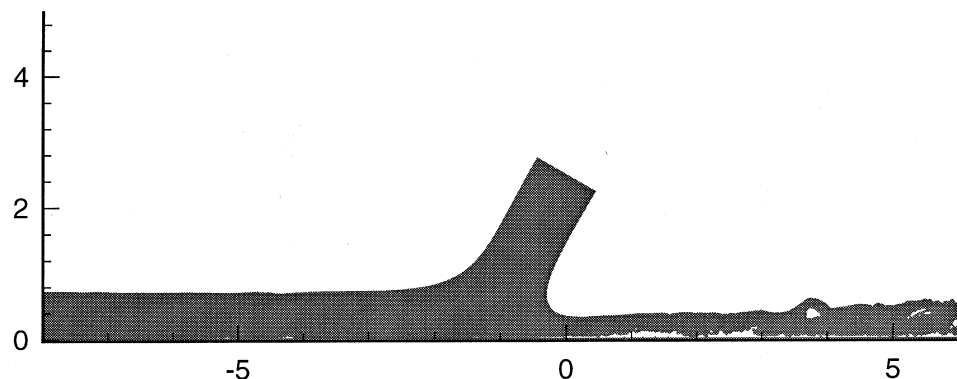


Fig. 5. Predicted flow patterns from SPH simulation of an impinging jet onto a moving surface, at  $Re=800$ , plate velocity (right to left)  $0.5$  times nozzle velocity;  $\theta=30^\circ$  (resolution approx. 35,000 particles),  $Fr=4.0$ .

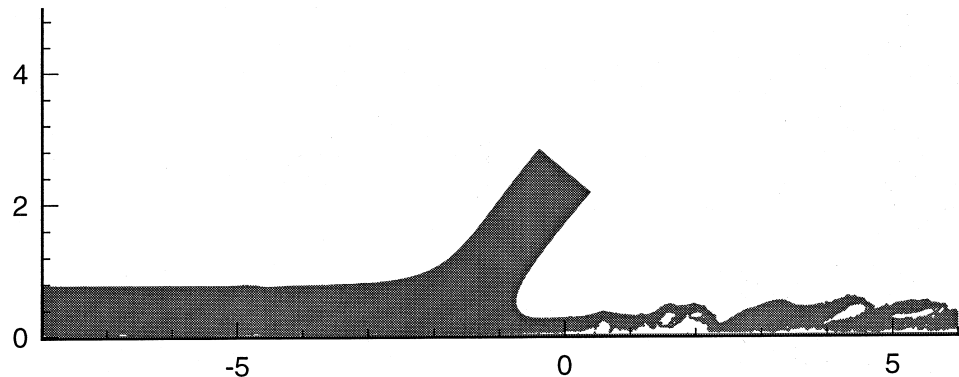


Fig. 6. Predicted flow patterns from SPH simulation of an impinging jet onto a moving surface, at  $Re = 800$ , plate velocity (right to left) 0.5 times nozzle velocity;  $\theta = 40^\circ$  (resolution approx. 35,000 particles),  $Fr = 4.0$ .



Fig. 7. Predicted flow patterns from SPH simulation at an early stage of development, of an impinging jet onto a moving surface, at  $Re = 50$ , plate velocity (right to left) 0.5 times nozzle velocity;  $\theta = 30^\circ$  (resolution approx. 95,000 particles),  $Fr = 4.0$ .



Fig. 8. Predicted flow patterns from SPH simulation at an impinging jet onto a moving surface, at  $Re = 50$ , plate velocity (right to left) 0.5 times nozzle velocity;  $\theta = 30^\circ$  (resolution approx. 70,000 particles),  $Fr = 1.0$ .

In this case undulations are observed in the thinner of the two streams, hence suggesting that the moving plate can cause some spatial variation in coating thickness. However an investigation involving a higher resolution in the thinner stream is required before any firm conclusions can be made. It should be noted that these results are awaiting experimental validation.

For all the cases listed above, the numerical results were obtained using a two-dimensional SPH model.

#### 4. Conclusions

SPH has been shown to predict well the heights of the streams associated with the impingement of a plane jet onto a stationary plate. The preliminary results, involving the impingement onto a moving plate, suggest that under such conditions spatial variation in the height of at least one of the streams can be observed.

### Nomenclature

$c$	speed of sound
$\text{dr}$	volume element
$F_{\text{ex}}$	external force
$\text{Fr}$	Froude number
$g$	gravity
$h$	smoothing length
$m_a$	mass of particle $a$
$P_0$	pressure equation constant
$P_a$	pressure at particle $a$
$\mathbf{r}_a$	position of particle $a$
$\text{Re}$	Reynolds number
$t$	time units
$\mathbf{V}_a$	velocity of particle $a$
$W(r,h)$	interpolating kernel
$\alpha, \beta$	artificial viscosity term constants
$\gamma$	power index in equation of state
$\mu_{ab}$	term in artificial viscosity equation
$\eta$	constant in artificial viscosity term
$\nabla$	spatial gradient
$\nabla_a$	spatial gradient taken with respect to coordinates of particle $a$
$\rho_0$	initial particle density
$\rho_a$	density of particle $a$
$\nu_{ab}$	viscosity acting between particle $a$ and $b$

### Acknowledgements

Paul Reichl would like to thank Monash University, and the Australian Postgraduate Award, which has funded this research.

### Appendix A

Bernoulli equation:

$$\frac{P_a}{\rho_a g} + \frac{v_a^2}{2g} + z_a = \frac{P_b}{\rho_b g} + \frac{v_b^2}{2g} + z_b.$$

Continuity equation:

$$\rho_{\text{in}} A_{\text{in}} \mathbf{v}_{\text{in}} = \sum_{\text{outlets}} \rho_{\text{out}} A_{\text{out}} \mathbf{v}_{\text{out}}.$$

$x$  momentum equation:

$$\rho_{\text{in}} \mathbf{v}_{\text{in}} A_{\text{in}} \mathbf{v}_{\text{in}} \sin \theta_* = \sum_{\text{outlets}} \rho_{\text{out}} A_{\text{out}} \mathbf{v}_{\text{out}} \mathbf{v}_{\text{out}}.$$

Here  $A_{\text{in}}$  and  $A_{\text{out}}$  are the widths of the inlet and outlets, respectively.

Applying these equations to the jet system results in four non-linear equations in four unknowns which can be solved numerically. Note that  $\theta_*$  refers to the angle of impingement corrected for the alteration caused by the fall under the effect of gravity.

## References

- [1] K.J. Ruscak, Coating Flows. *Ann. Rev. Fluid Mech.* 17 (1985) 65–89.
- [2] L. Lucy, A numerical approach to the testing of the fission hypothesis. *Astron. J.* 82 (1977) 1013–1024.
- [3] R.A. Gingold, J.J. Monaghan, Smoothed particle hydrodynamics: Theory and application to non spherical stars, *Monthly Notices of the Royal Astrophysical Society* 181 (1977) 375–389.
- [4] J.J. Monaghan, Simulating free surface flows with SPH, *Journal of Computational Physics* 110 (1994) 399–406.
- [5] M.C. Thompson, K. Hourigan, J.J. Monaghan, Simulation of free surface flows with SPH, in: *Advances in Computational Methods in Fluid Mechanics 1994*, The 1994 ASME Fluids Engineering Division Summer Meeting, Lake Tahoe, Nevada, 19–23 June 1994.
- [6] H. Takeda, S.M. Miyama, M. Sekiya, Numerical simulation of viscous flow by smoothed particle hydrodynamics, *Progress of Theoretical Physics* 92 (1994) 939–960.
- [7] L.D. Cloutman, An evaluation of smoothed particle hydrodynamics, in: H.E. Trease, M.J. Fritts, W.P. Crowley (Eds.), *Advances in the Free-Lagrange Method*, Springer, Berlin, 1991, pp. 229–247.
- [8] J.J. Monaghan, Smoothed particle hydrodynamics, *Annu. Rev. Astron. Astrophys.* 30 (1992) 543–574.
- [9] J.R. Murray, SPH simulation of accretion disks in cataclysmic variables, Ph.D. Thesis, Monash University, 1995.
- [10] S.J. Watkins, A.S. Bhattacharjee, N. Francis, J.A. Turner, A.P. Whitworth, A new prescription for viscosity in SPH, *A&ASS* 119 (1996) 177–188.
- [11] G.K. Batchelor, *An Introduction to Fluid Mechanics*, Cambridge Press, London, 1967, p. 615.
- [12] J.J. Monaghan, J.C. Lattanzio, A refined particle method for astrophysical problems, *Astronomy and Astrophysics* 149 (1985) 135–143.
- [13] J.P.A. Morris, An overview on the method of smooth particle hydrodynamics, Private communication, 1996.